Memory Wrap: a Data-Efficient and Interpretable Extension to Image Classification Models

Biagio La Rosa* Sapienza University larosa@diag.uniroma1.it Roberto Capobianco Sapienza University Sony AI capobianco@diag.uniroma1.it

Daniele Nardi

Sapienza University nardi@diag.uniroma1.it

Abstract

Due to their black-box and data-hungry nature, deep learning techniques are not yet widely adopted for real-world applications in critical domains, like healthcare and justice. This paper presents Memory Wrap, a plug-and-play extension to any image classification model. Memory Wrap improves both data-efficiency and model interpretability, adopting a content-attention mechanism between the input and some memories of past training samples. We show that Memory Wrap outperforms standard classifiers when it learns from a limited set of data, and it reaches comparable performance when it learns from the full dataset. We discuss how its structure and content-attention mechanisms make predictions interpretable, compared to standard classifiers. To this end, we both show a method to build explanations by examples and counterfactuals, based on the memory content, and how to exploit them to get insights about its decision process. We test our approach on image classification tasks using several architectures on three different datasets, namely CIFAR10, SVHN and CINIC10.

1 Introduction

In the last decade, Artificial Intelligence has seen an explosion of applications thanks to advancements in deep learning techniques. Despite their success, these techniques suffer from some important problems: they require a lot of data to work well, and they act as black boxes, taking an input and returning an output without providing any explanation about that decision. The lack of transparency limits the adoption of deep learning in important domains like health-care and justice, while the data requirement makes harder its generalization on real-world tasks. Few-shot learning methods and explainable artificial intelligence (XAI) approaches address these problems. The former studies the data requirement, experimenting on a type of machine learning problem where the model can only use a limited number of samples; the latter studies the problem of transparency, aiming at developing methods that can explain, at least partially, the decision process of neural networks. While there is an extensive literature on each topic, few works explore methods that can be used both on low data regime and that can provide explanations about their outputs.

This paper makes a little step in both directions, proposing Memory Wrap, an approach that makes image classification models more data-efficient by providing, at the same time, a way to inspect their decision process. In classical settings of supervised learning, models use the training set only to

^{*}Contact Author

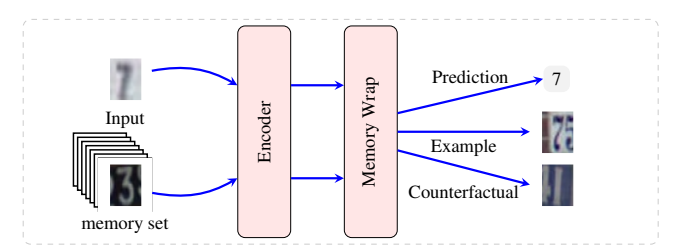


Figure 1: Overview of Memory Wrap. The encoder takes as input an image and a memory set, containing random samples extracted from the training set. The encoder sends their latent representations to Memory Wrap, which outputs the prediction, an explanation by example, and a counterfactual, exploiting the sparse content attention between inputs encodings.

adjust their weights, discarding it at the end of the training process. Instead, we hypothesize that, in a low data regime, it is possible to strengthen the learning process by re-using samples from the training set during inference. Taking inspiration from Memory Augmented Neural Networks [6, 25], the idea is to store a bunch of past training samples (called *memory set*) and combine them with the current input through sparse attention mechanisms to help the neural network decision process. Since the network actively uses these samples during inference, we propose a method based on inspection of sparse content attention weights to extract insights and explanations about its predictions.

We test our approach on image classification tasks using CIFAR10 [13], Street View House Number (SVHN) [21], and CINIC10 [4] obtaining promising results. Our contribution can be summarized as follows:

- we present Memory Wrap, an extension for image classification models that uses a memory containing past training examples to enrich the input encoding;
- we show it makes the original model more data-efficient, achieving higher accuracy on low data regimes;
- we discuss methods to make their predictions more interpretable. In particular, we show that not only it is possible to extract the samples that actively contribute to the prediction, but we can also measure how much they contribute. Additionally, we show a method to retrieve similar examples from the memory that allow us to inspect which features are important for the current prediction, in the form of explanation by examples and counterfactuals.

The manuscript is organized as follows. Section 2 reviews existing literature, focusing on works that use similar methods to us and discuss the state-of-the-art in network explainability; Section 3 introduces our approach, while Section 4 presents some experiments and their results. Finally, we discuss conclusions, limitations and future directions.

2 Background

2.1 Memory Augmented Neural Networks

Our work has been inspired by current advances in Memory Augmented Neural Networks (MANNs) [6, 7, 14, 25]. MANNs use an external memory to store and retrieve data during input processing. They can store past steps of a sequence, as in the case of recurrent architectures for sequential tasks, or they can store external knowledge in form of a knowledge base [5]. Usually, the network interacts with the memory through attention mechanisms, and it can also learn how to write and read the memory during the training process [6]. Differentiable Neural Computers [7] and End-To-End Memory Networks [25] are popular examples of this class of architectures. Researchers apply them to several problems like visual question answering [19], image classification [2], and meta-learning [23], reaching great results.

Similarly to MANNs, Matching Networks [29] use a set of *never seen before* samples to boost the learning process of a new class in one-shot classification tasks. Differently from us, their architecture is standalone and it applies the product of attention mechanisms on the labels of the sample set in order to compute the final prediction. Conversely, Prototypical Networks [24] use samples of

the training set to perform metric learning and to return predictions based on the distance between prototypes in the embedding space and the current input. Our approach relies on similar ideas, but it uses a memory set that contains *already seen and already learned* examples in conjunction with a sparse attention mechanism. While we adopt a similarity measure to implement our attention mechanism, we do not use prototypes or learned distances: the network itself learns to choose which features should be retrieved from each sample and which samples are important for a given input. Moreover, our method differs from Prototype Networks because it is model agnostic and can be potentially applied to any image classification model without modifications.

2.2 Explainable Artificial Intelligence

Lipton [16] distinguishes between *transparent models*, where one can unfold the chain of reasoning (e.g. decision trees), and *post-hoc explanations*, that explain predictions without looking inside the neural network. The last category includes explanation by examples and counterfactuals, which are the focus of our method.

Explanations by examples aim at extracting representative instances from given data to show how the network works [1]. Ideally, the instances should be similar to the input and, in classification settings, predicted in the same class. In this way, by comparing the input and the examples, a human can extract both similarities between them and features that the network uses to return answers.

Counterfactuals are specular to explanations by examples: the instances, in this case, should be similar to the current input but classified in another class. By comparing the input to counterfactuals, it is possible to highlight differences and to extract edits that should be applied to the current input to obtain a different prediction. While for tabular data it is feasible to get counterfactuals by changing features and at the same time to respect domain constraints [20], for images and natural language processing the task is more challenging. This is due to the lack of formal constraints and to the extremely large range of features to be changed.

Recent research on explanation by examples and counterfactuals adopts search methods [30, 18], which have high latency due to the large search space, and Generative Adversarial Networks (GANs). For example, Liu *et al.* [17] use GANs to generate counterfactuals for images, but – since they are black-boxes themselves – it is difficult to understand why a particular counterfactual is a good candidate or not.

For small problems, techniques like KNN and SVM [3] can easily compute neighbors of the current input based on distance measures, and use them as example-based explanations. Unfortunately, for problems involving a large number of features and neural networks, it becomes less trivial to find a correct distance metric that both takes into account the different feature importance and that is effectively linked to the neural network decision process. An attempt in this direction is the twinsystem proposed by Kenny and Keane [11], which combines case-based reasoning systems (CBR) and neural networks. The idea is to map the latent space or neural weights to white-box case-based reasoners and extract from them explanations by examples. With respect to these approaches, our method is intrinsic, meaning that is embedded inside the architecture and, more importantly, it is directly linked to the decision process, actively contributing to it. Our method does not require external architectures like GANs or CBR and it does not have any latency associated with its use.

3 Memory Wrap

This section describes the architecture of Memory Wrap and a methodology to extract example-based explanations and counterfactuals for its predictions.

3.1 Architecture

Memory Wrap extends existing classifiers, specialized in a given task, by replacing the last layer of the model. Specifically, it includes a sparse content-attention mechanism and a multi-layer perceptron that work together to exploit the combination of an input and a bunch of training samples. In this way, the pre-existent model acts as an *encoder*, focused on extracting input features and mapping them into a latent space. Memory Wrap stores previous examples (*memories*) that are then used at inference time. The only requirement for the encoder is that its last layer – before the Memory Wrap

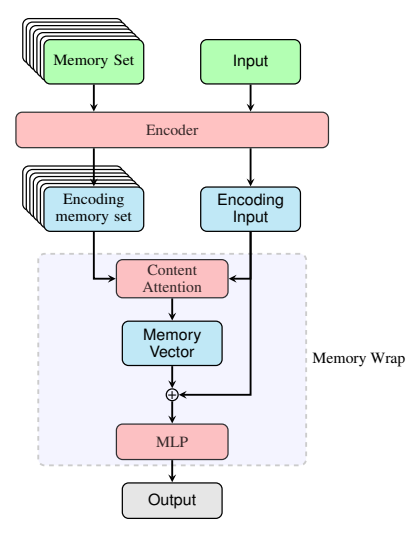


Figure 2: Sketch of the system architecture. The system encodes the input and a bunch of training samples using a chosen neural network. Then, it generates a memory vector as a weighted sum of the memory set based on the sparse content attention weights between the encodings. Finally, the last layer predicts the input class, taking as input the concatenation of the memory vector and the input encoding.

– outputs a vector containing a latent representation of the input. Clearly, the structure of the encoder impacts on the representation power, so we expect that a better encoder architecture could improve further the performance of Memory Wrap.

More formally, let be g(x) the whole model, f(x) the encoder, x_i the current input, and $S_i = \{x_{m_1}^i, x_{m_2}^i, ..., x_{m_n}^i\}$ a set of n samples called *memory set*, randomly extracted from the training set during the current step i. First of all, the encoder f(x) encodes both the input and the memory set, projecting them in the latent space and returning respectively:

$$e_{x_i} = f(x_i) \qquad \mathbf{M}_{S_i} = \{m_1^i, m_2^i, ..., m_n^i\} = \{f(x_{m_1}^i), f(x_{m_2}^i), ..., f(x_{m_n}^i)\}.$$
 (1)

Then, Memory Wrap computes the sparse content attention weights as the sparsemax [22] of the similarity between the input encoding and memory set encodings, thus attaching a content weight w_j to each encoded sample m_j^i . We compute content attention weights using the cosine similarity as in Graves *et al.* [7], replacing the softmax function with a sparsemax.

$$\mathbf{w} = sparsemax(cosine[e_{x_i}, \mathbf{M}_{S_i}]). \tag{2}$$

Since we are using the sparsemax function, the memory vector only includes information from few samples of the memory. In this way, each sample contributes in a significant way, helping us to achieve output explainability. Similarly to [7], we compute the *memory vector* $\mathbf{v}_{\mathbf{S_i}}$ as the weighted sum of memory set encodings, where the weights are the content attention weights:

$$\mathbf{v}_{\mathbf{S}_{i}} = \mathbf{M}_{S_{i}}^{T} \mathbf{w}. \tag{3}$$

Finally, the last layer l_f takes the concatenation of the memory vector and the encoded input, and returns the final output

$$o_i = g(x_i) = l_f([e_i(x_i), \mathbf{v_{S_i}}]). \tag{4}$$

The role of the memory vector is to enrich the input encoding with *additional* features extracted from similar samples, possibly missing on the current input. On average, considering the whole memory set and thanks to the cosine similarity, strong features of the target class will be more represented than features of other classes, helping the network in the decision process. In our case, we use a multi-layer perceptron with only one hidden layer as a final layer, but other choices are possible (App. A.2).

3.2 Getting explanations

We aim at two types of explanations: explanation by examples and counterfactuals. The idea is to exploit the memory vector and content attention weights to extract explanations about model outputs, in a similar way to La Rosa et~al. [15]. To understand how, let's consider the current input x_i , the current prediction $g(x_i)$, and the encoding matrix M_{S_i} of the memory set, where each $m_j^i \in M_{S_i}$ is associated with a weight w_j . We can split the matrix M_{S_i} into three disjoint sets $M_{S_i} = M_e \cup M_c \cup M_z$, where $M_e = \{f(x_{m_j}^i) \mid g(x_i) = g(x_{m_j}^i)\}$ contains encodings of samples predicted in the same class $g(x_i)$ by the network and associated with a weight $w_j > 0$, $M_c = \{f(x_{m_j}^i) \mid g(x_i) \neq g(x_{m_j}^i)\}$ contains encodings of samples predicted in a different class and associated with a weight $w_j > 0$, and M_z contains encodings of samples associated with a weight $w_j = 0$. Note that this last set does not contribute at all to the decision process and it cannot be considered for explainability purposes. Conversely, since M_e and M_c have positive weights, they can be used to extract explanation by examples and counterfactuals.

Let's consider, for each set, the sample $x^i_{m_j}$ associated with the highest weight. A high weight of w_j means that the encoding of the input x_i and the encoding of the sample $x^i_{m_j}$ are similar. If $x^i_{m_j} \in M_e$, then it can be considered as a good candidate for an explanation by example, being an instance similar to the input and predicted in the same class, as defined in Sect. 2.2. Instead, if $x^i_{m_j} \in M_c$, then it is considered as a counterfactual, being similar to the input but predicted in a different class. Finally, consider the sample $x^i_{m_k}$ associated with the highest weight in the whole set M_{S_i} . Because it is the highest, it will be heavily represented in the memory vector that will **actively** contribute to the inference, being used as input for the last layer. This means that common features between the input and the sample $x^i_{m_k}$ are highly represented and so they constitute a good explanation. Moreover, if $x^i_{m_k}$ was a counterfactual, because it is partially included in the memory vector, it is likely that it will be the second or third predicted class, giving also information about "doubts" of the neural network.

4 Results

This section first describes the experimental setups, and then it presents and analyzes the obtained results for both performance and explanations.

4.1 Setup

We test our approach on image classification tasks using the Street View House Number (SVHN) [21], CINIC10 [4] and CIFAR10 [13] datasets. For the encoder f(x), we run our tests using ResNet18 [8], EfficientNet B0 [28], MobileNet-v2 [9], and other architectures whose results are reported in App. A.5. We randomly split the training set to extract smaller sets in the range $\{1000,2000,5000\}$, thus simulating a low regime data setting, and then train each model using these sets and the whole dataset. At each training step, we randomly extract 100 samples from the training set and we use them as memory set — \sim 10 samples for each class (see App. A.7 and App. A.6 for further details about this choice). We run 15 experiments for each configuration, fixing the seeds for each run and therefore training each model under identical conditions. We report the mean accuracy and the standard deviation over the 15 runs for each model and dataset. For further details about the training setup please consult App. A.1.

4.1.1 Baselines

Standard. This baseline is obtained with the classifiers f(x) without any modification and trained in the same manner of Memory Wrap (i.e. same settings and seeds).

Only Memory. This baseline uses only the memory vector as input of the multi-layer perceptron, removing the concatenation with the encoded input. Therefore, the output is given by $o_i = g(x_i) = l_f(\mathbf{v}_{\mathbf{S}_i})$. In this case, the input is used only to compute the content weights, which are then used to build the memory vector, and the network learns to predict the correct answer based on them. Because of the randomness of the memory set and the absence of the encoded input image as input of the last layer, the network is encouraged to learn more general patterns and not to exploit specific features of the given image.

Table 1: Avg. accuracy and standard deviation over 15 runs of the baselines and Memory Wrap, when the training dataset is a subset of SVHN. For each configuration, we highlight in bold the best result and results that are within its margin.

Reduced SVHN Avg. Accuracy%				
Samples				
Model	Variant	1000	2000	5000
EfficientNetB0	Standard	57.70 ± 7.89	72.59 ± 4.00	81.89 ± 3.37
	Only Memory	58.86 ± 3.30	75.79 ± 1.68	$\textbf{85.30} \pm \textbf{0.52}$
	Memory Wrap	$\textbf{66.78} \pm \textbf{1.27}$	$\textbf{77.37} \pm \textbf{1.25}$	$\textbf{85.55} \pm \textbf{0.59}$
MobileNet-v2	Standard	42.71 ± 10.31	70.87 ± 4.20	85.52 ± 1.16
	Only Memory	60.60 ± 3.14	$\textbf{80.80} \pm \textbf{2.05}$	$\textbf{88.77} \pm \textbf{0.42}$
	Memory Wrap	$\textbf{66.93} \pm \textbf{3.15}$	$\textbf{81.44} \pm \textbf{0.76}$	$\textbf{88.68} \pm \textbf{0.46}$
ResNet18	Standard	20.63 ± 2.85	31.84 ± 18.38	79.03 ± 12.89
	Only Memory	35.57 ± 6.48	68.87 ± 8.70	$\textbf{87.63} \pm \textbf{0.42}$
	Memory Wrap	$\textbf{45.31} \pm \textbf{8.19}$	$\textbf{77.26} \pm \textbf{3.38}$	$\textbf{87.74} \pm \textbf{0.35}$

Table 2: Avg. accuracy and standard deviation over 15 runs of the baselines and Memory Wrap, when the training dataset is a subset of CIFAR10. For each configuration, we highlight in bold the best result and results that are within its margin.

Reduced CIFAR10 Avg. Accuracy%				
			Samples	
Model	Variant	1000	2000	5000
EfficientNetB0	Standard	39.63 ± 2.16	47.25 ± 2.22	67.34 ± 2.37
	Only Memory	40.60 ± 2.04	$\textbf{52.87} \pm \textbf{2.07}$	$\textbf{70.82} \pm \textbf{0.52}$
	Memory Wrap	$\textbf{41.45} \pm \textbf{0.79}$	$\textbf{52.83} \pm \textbf{1.41}$	$\textbf{70.46} \pm \textbf{0.78}$
MobileNet-v2	Standard	38.57 ± 2.11	50.36 ± 2.64	72.77 ± 2.21
	Only Memory	$\textbf{43.15} \pm \textbf{1.35}$	$\textbf{57.43} \pm \textbf{1.45}$	$\textbf{75.56} \pm \textbf{0.76}$
	Memory Wrap	$\textbf{43.87} \pm \textbf{1.40}$	$\textbf{57.12} \pm \textbf{1.36}$	$\textbf{75.33} \pm \textbf{0.62}$
ResNet18	Standard	$\textbf{40.03} \pm \textbf{1.36}$	48.86 ± 1.57	65.95 ± 1.77
	Only Memory	$\textbf{40.35} \pm \textbf{0.89}$	$\textbf{51.11} \pm \textbf{1.22}$	$\textbf{70.28} \pm \textbf{0.80}$
	Memory Wrap	$\textbf{40.91} \pm \textbf{1.25}$	$\textbf{51.11} \pm \textbf{1.13}$	$\textbf{69.87} \pm \textbf{0.72}$

Table 3: Avg. accuracy and standard deviation over 15 runs on SVHN dataset of the baselines and Memory Wrap. The comparison highlights the difference in performance when using a subset of the dataset in the range {1k,2k,5k} as training set. For each configuration, we highlight in bold the best result and results that are within its margin.

Reduced CINIC10 Avg. Accuracy%					
Samples					
Model	Variant	1000	2000	5000	
EfficientNetB0	Standard	29.50 ± 1.18	33.56 ± 1.26	45.98 ± 1.34	
	Only Memory	$\textbf{30.46} \pm \textbf{1.17}$	$\textbf{36.17} \pm \textbf{1.54}$	44.97 ± 0.95	
	Memory Wrap	$\textbf{30.45} \pm \textbf{0.64}$	$\textbf{36.65} \pm \textbf{1.03}$	$\textbf{47.06} \pm \textbf{0.91}$	
MobileNet-v2	Standard	29.61 ± 0.89	36.40 ± 1.58	50.41 ± 1.01	
	Only Memory	$\textbf{32.46} \pm \textbf{1.07}$	$\textbf{39.91} \pm \textbf{0.82}$	$\textbf{52.51} \pm \textbf{0.77}$	
	Memory Wrap	$\textbf{32.34} \pm \textbf{0.95}$	$\textbf{39.48} \pm \textbf{1.16}$	$\textbf{52.18} \pm \textbf{0.66}$	
ResNet18	Standard	31.18 ± 1.21	37.67 ± 0.98	45.39 ± 1.07	
	Only Memory	30.79 ± 0.83	37.30 ± 0.57	$\textbf{46.66} \pm \textbf{0.81}$	
	Memory Wrap	$\textbf{32.15} \pm \textbf{0.68}$	$\textbf{38.51} \pm \textbf{0.96}$	$\textbf{46.39} \pm \textbf{0.67}$	

4.2 Performance

In low data regimes, our method outperforms the standard models in all the datasets, sometimes with a large margin (Table 1, Table 3, and Table 2). First, we can observe that the amount of gain in performance depends on the used encoder: MobileNet shows the largest gap in all the datasets, while ResNet shows the smallest one, representing a challenging model for Memory Wrap. Secondly, it depends on the dataset, being the gains in each SVHN configuration always greater than the ones in CIFAR10 and CINIC10. Regarding the baseline that uses only the memory, it outperforms the standard baseline too, reaching nearly the same performance of Memory Wrap in most of the settings. However, its performance appears less stable across configurations, being lower than Memory Wrap in some SVHN and CINIC10 settings (Table 1 and Table 3) and lower than standard models in some full dataset scenarios and in some configurations of CINIC10. These considerations are confirmed also on other architectures reported in App. A.5. We hypothesize that the additional information captured by the input encoding allow the model to exploit additional shortcuts and to reach the best performance.

Note that it is possible to increase the gap by adding more samples in the memory, at the cost of an increased training and inference time (App. A.7). Moreover, while in low data regimes standard neural networks performances show high variance, Memory Wrap seems to be a lot more stable with a lower standard deviation.

When Memory Wrap learns from the full dataset (Table 4), it reaches comparable performance most of the time. Hence, our approach is useful also when used with the full dataset, thanks to the additional interpretability opportunity provided by its structure (Section 3.2).

4.3 Explanations

From now on, we will consider MobileNet-v2 as our base network, but the results are similar for all the considered models and configurations (App. A.4 and A.8). The first step that we can do to extract insights about the decision process, is to check which samples in the memory set have positive weights – the set $M_c \cup M_e$. Figure 3 shows this set ordered by the magnitude of content weights for four different inputs: each couple shares the same memory set as additional input, but each set of used samples – those associated with a positive weight – is different. In particular, consider the images in Figure 3a, where the only change is a lateral shift made to center different numbers. Despite their closeness in the input space, samples in memory are totally different: the first set contains images of "5" and "3", while the second set contains mainly images of "1" and few images of "7". We can infer that probably the network is focusing on the shape of the number in the center to classify the image, ignoring colors and the surrounding context. Conversely, in Figure 3b the top samples in memory are images with similar colors and different shapes, telling us that the network is wrongly focusing on the association between color in the background and color of the object in the center. This means that the inspection of samples in the set $M_c \cup M_e$ can give us some insights about the decision process.

Table 4: Avg. accuracy and standard deviation over 15 runs of the baselines and Memory Wrap, when the training datasets are the whole SVHN and CIFAR10 datasets. For each configuration, we highlight in bold the best result and results that are within its margin.

Full Datasets Avg. Accuracy %						
Model	Variant	SVHN	CIFAR10	CINIC10		
EfficientNetB0	Standard Only Memory Memory Wrap	$\textbf{94.63} \pm \textbf{0.33}$		76.19 ± 0.25		
MobileNet-v2	Standard Only Memory Memory Wrap	95.59 ± 0.11		74.60 ± 0.13		
ResNet18	Standard Only Memory Memory Wrap	$\textbf{95.82} \pm \textbf{0.10}$		81.65 ± 0.19		

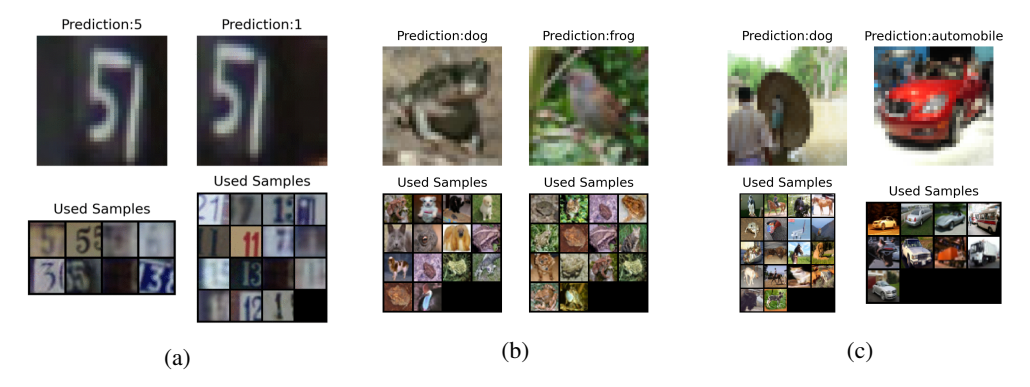


Figure 3: Inputs (first rows), their associated predictions and an overview of the samples in the memory set that have an active influence on the decision process - i.e. the samples on which the memory vector is built - (second row).

Once we have defined the nature of the samples in the memory set that influence the inference process, we can check whether the content weight ranking is meaningful for Memory Wrap predictions. To verify that this is the case, consider the most represented sample inside the memory vector (i.e. the sample $x_{m_k}^i$ associated with the highest content weight). Then, let $g(x_{m_k}^i)$ be the prediction obtained by replacing the current input with this sample, and the current memory set S_i with a new one. If

Table 5: Mean Explanation accuracy and standard deviation over 15 runs of the sample in the memory set with the highest sparse content attention weight.

	Explanation Accuracy %					
Dataset	Samples	Only Memory	Memory Wrap			
SVHN	1000	81.46 ± 1.05	84.26 ± 1.29			
	2000	89.53 ± 1.05	90.76 ± 0.50			
	5000	93.79 ± 0.23	94.56 ± 0.20			
CIFAR10	1000	77.81 ± 0.93	78.03 ± 0.81			
	2000	82.39 ± 0.65	82.01 ± 0.49			
	5000	89.17 ± 0.34	88.49 ± 0.26			
CINIC10	1000	75.99 ± 0.80	76.30 ± 0.75			
	2000	78.38 ± 0.46	78.43 ± 0.55			
	5000	80.90 ± 0.33	74.47 ± 0.62			

Table 6: Accuracy reached by the model on images where the sample with the highest weight in memory set is a counterfactual. The accuracy is computed as the mean over 15 runs using as encoder MobileNet-v2.

Accuracy %					
Dataset	Samples	Only Memory	Memory Wrap		
SVHN	1000	35.45 ± 2.47	39.90 ± 1.84		
	2000	43.79 ± 1.20	45.60 ± 1.08		
	5000	48.02 ± 1.02	49.02 ± 1.39		
CIFAR10	1000	30.56 ± 1.08	31.78 ± 0.82		
	2000	36.93 ± 0.83	37.15 ± 0.70		
	5000	44.57 ± 1.19	45.80 ± 0.77		
CINIC10	1000	25.20 ± 0.57	25.36 ± 0.62		
	2000	28.77 ± 0.42	28.70 ± 0.59		
	5000	34.18 ± 0.56	35.22 ± 0.46		

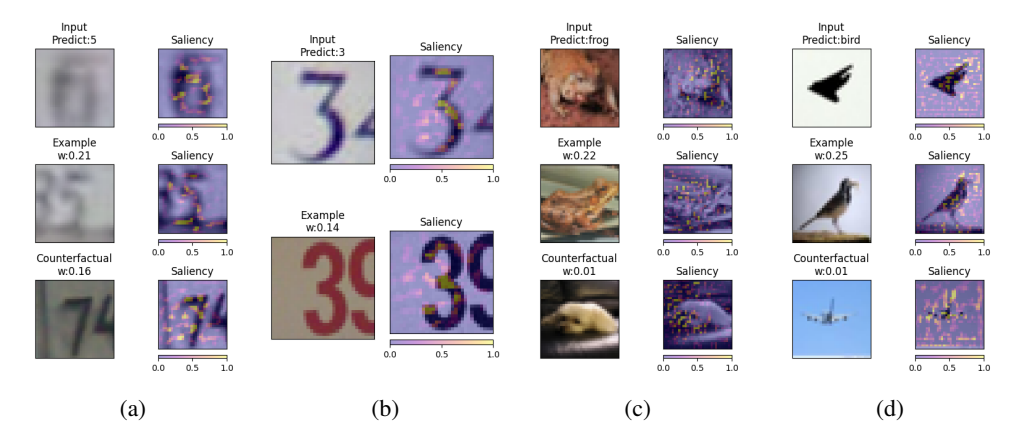


Figure 4: Integrated Gradients heatmaps of the input, the explanation by example associated with the highest weight in memory, and (eventually) the counterfactual associated with the highest weight. Each heatmap highlights the pixels that have a positive impact towards the current prediction.

the sample influences in a significant way the decision process and if it can be considered as a good proxy for the current prediction $g(x_i)$ (i.e a good explanation by example), then $g(x_{m_k}^i)$ should be equal to $g(x_i)$. Therefore, we set the *explanation accuracy* as a measure that checks how many times the sample in the memory set with the highest weight is predicted in the same class of the current image. Table 5 shows the explanation accuracy of MobileNet-v2 in all the considered configurations. We observe that Memory Wrap reaches high accuracy, meaning that the content weights ranking is reliable. Additionally, its accuracy is very close to the baseline that uses only the memory, despite the fact this latter is favored by its design, meaning that the memory content heavily influences the decision process.

Clearly, the same test cannot be applied to counterfactuals, because, by construction, they are samples of a different class. However, we can inspect what happens when a counterfactual is the sample with the highest weight. We find (Table 6) that the model accuracy is much lower in these cases, meaning that its predictions are often wrong and one can use this information to alert the user that the decision process could be unreliable.

Since the memory is actively used during the inference phase, we can use attribution methods to extract further insights about the decision process (see App. A.3 for a discussion about the choice of the attribution method). For example, Figure 4 shows heatmaps obtained applying Integrated Gradients² [26], a method that highlights the most relevant pixels for the current prediction, exploiting the gradients. For both Figure 4a and Figure 4d, the model predicts the wrong class. In the 4d case, the heatmap of the explanation by example tells us that the model focuses on bird and sky colors, ignoring the unusual shape of the airplane, very different from previously known shapes for airplanes, which are represented by the counterfactual with a very low weight and a heatmap that focuses only on the sky. Conversely in the 4c case, the model ignores colors and focuses on the head shape, a feature that is highlighted both in the input image and in the explanations. Finally, sometimes (see Figure 4b) counterfactuals are missing, and this means that the model is sure about its prediction and it uses only examples of the same class.

5 Conclusion and future research

In this paper, we presented an extension for neural networks that allows a more efficient use of the training dataset in settings where few data are available. Moreover, we propose an approach to extract explanations based on similar examples and counterfactuals.

Future work could explore the reduction of current limitations, like the memory space needed to store the memory samples and their gradients (App. A.6). Another limitation is that the memory mechanism based on similarity could amplify the bias learned by the encoder. As shown in Sect. 3.2, the identification of such an event is straightforward, but currently there are not countermeasures

²We use the Captum library [12]

against it. A new adaptive or algorithmic selection mechanism of memory samples or a regularization method could mitage the bias and it could improve the fairness of Memory Wrap. Finally, the findings of this paper open up also possible extensions on different problems like semi-supervised learning, where the self uncertainty detection of Memory Wrap could be useful, and domain adaption.

Acknowledgments and Disclosure of Funding

This material is based upon work supported by Google Cloud.

References

- [1] Vaishak Belle and Ioannis Papantonis. Principles and practice of explainable machine learning. 2020.
- [2] Qi Cai, Yingwei Pan, Ting Yao, Chenggang Yan, and Tao Mei. Memory matching networks for one-shot image recognition. In 2018 IEEE/CVF Conference on Computer Vision and Pattern Recognition. IEEE, 2018.
- [3] Corinna Cortes and Vladimir Vapnik. Support-vector networks. *Machine Learning*, 20(3):273–297, 1995.
- [4] Luke N. Darlow, Elliot J. Crowley, Antreas Antoniou, and Amos J. Storkey. Cinic-10 is not imagenet or cifar-10. October 2018.
- [5] Emily Dinan, Stephen Roller, Kurt Shuster, Angela Fan, Michael Auli, and Jason Weston. Wizard of wikipedia: Knowledge-powered conversational agents. 2018.
- [6] Alex Graves, Greg Wayne, and Ivo Danihelka. Neural turing machines. 2014.
- [7] Alex Graves, Greg Wayne, Malcolm Reynolds, Tim Harley, Ivo Danihelka, Agnieszka Grabska-Barwińska, Sergio Gómez Colmenarejo, Edward Grefenstette, Tiago Ramalho, John Agapiou, Adrià Puigdomènech Badia, Karl Moritz Hermann, Yori Zwols, Georg Ostrovski, Adam Cain, Helen King, Christopher Summerfield, Phil Blunsom, Koray Kavukcuoglu, and Demis Hassabis. Hybrid computing using a neural network with dynamic external memory. *Nature*, 538(7626):471–476, 2016.
- [8] Kaiming He, Xiangyu Zhang, Shaoqing Ren, and Jian Sun. Deep residual learning for image recognition. In 2016 IEEE Conference on Computer Vision and Pattern Recognition (CVPR). IEEE, 2016.
- [9] Andrew G. Howard, Menglong Zhu, Bo Chen, Dmitry Kalenichenko, Weijun Wang, Tobias Weyand, Marco Andreetto, and Hartwig Adam. Mobilenets: Efficient convolutional neural networks for mobile vision applications. 2017.
- [10] Gao Huang, Zhuang Liu, Laurens Van Der Maaten, and Kilian Q. Weinberger. Densely connected convolutional networks. In 2017 IEEE Conference on Computer Vision and Pattern Recognition (CVPR). IEEE, 2017.
- [11] Eoin M. Kenny and Mark T. Keane. Twin-systems to explain artificial neural networks using case-based reasoning: Comparative tests of feature-weighting methods in ANN-CBR twins for XAI. In *Proceedings of the Twenty-Eighth International Joint Conference on Artificial Intelligence*. International Joint Conferences on Artificial Intelligence Organization, 2019.
- [12] Narine Kokhlikyan, Vivek Miglani, Miguel Martin, Edward Wang, Bilal Alsallakh, Jonathan Reynolds, Alexander Melnikov, Natalia Kliushkina, Carlos Araya, Siqi Yan, and Orion Reblitz-Richardson. Captum: A unified and generic model interpretability library for pytorch. 2020.
- [13] A. Krizhevsky. Learning multiple layers of features from tiny images. 2009.
- [14] Ankit Kumar, Ozan Irsoy, Peter Ondruska, Mohit Iyyer, James Bradbury, Ishaan Gulrajani, Victor Zhong, Romain Paulus, and Richard Socher. Ask me anything: Dynamic memory networks for natural language processing. In *Proceedings of the 33rd International Conference on International Conference on Machine Learning*, volume 48 of *ICML'16*, page 1378–1387. JMLR.org, 2016.

- [15] Biagio La Rosa, Roberto Capobianco, and Daniele Nardi. Explainable inference on sequential data via memory-tracking. In *Proceedings of the Twenty-Ninth International Joint Conference* on Artificial Intelligence. International Joint Conferences on Artificial Intelligence Organization, 2020.
- [16] Zachary C. Lipton. The mythos of model interpretability: In machine learning, the concept of interpretability is both important and slippery. Queue, 16(3):31–57, 2018.
- [17] Shusen Liu, Bhavya Kailkhura, Donald Loveland, and Yong Han. Generative counterfactual introspection for explainable deep learning. 2019.
- [18] Arnaud Van Looveren and Janis Klaise. Interpretable counterfactual explanations guided by prototypes. 2019.
- [19] Chao Ma, Chunhua Shen, Anthony Dick, Qi Wu, Peng Wang, Anton van den Hengel, and Ian Reid. Visual question answering with memory-augmented networks. In 2018 IEEE/CVF Conference on Computer Vision and Pattern Recognition. IEEE, 2018.
- [20] Divyat Mahajan, Chenhao Tan, and Amit Sharma. Preserving causal constraints in counterfactual explanations for machine learning classifiers. 2019.
- [21] Yuval Netzer, Tao Wang, Adam Coates, Alessandro Bissacco, Bo Wu, and Andrew Y. Ng. Reading digits in natural images with unsupervised feature learning. In NIPS Workshop on Deep Learning and Unsupervised Feature Learning 2011, 2011.
- [22] Ben Peters, Vlad Niculae, and André F. T. Martins. Sparse sequence-to-sequence models. In *Proceedings of the 57th Annual Meeting of the Association for Computational Linguistics*. Association for Computational Linguistics, 2019.
- [23] Adam Santoro, Sergey Bartunov, Matthew Botvinick, Daan Wierstra, and Timothy Lillicrap. Meta-learning with memory-augmented neural networks. volume 48 of *Proceedings of Machine Learning Research*, pages 1842–1850. PMLR, 2016.
- [24] Jake Snell, Kevin Swersky, and Richard Zemel. Prototypical networks for few-shot learning. In Proceedings of the 31st International Conference on Neural Information Processing Systems, NIPS'17, page 4080–4090. Curran Associates Inc., 2017.
- [25] Sainbayar Sukhbaatar, Arthur Szlam, Jason Weston, and Rob Fergus. End-to-end memory networks. In *Proceedings of the 28th International Conference on Neural Information Processing* Systems - Volume 2, NIPS'15, page 2440–2448. MIT Press, 2015.
- [26] Mukund Sundararajan, Ankur Taly, and Qiqi Yan. Axiomatic attribution for deep networks. In Proceedings of the 34th International Conference on Machine Learning - Volume 70, ICML'17, page 3319–3328. JMLR.org, 2017.
- [27] Christian Szegedy, Wei Liu, Yangqing Jia, Pierre Sermanet, Scott Reed, Dragomir Anguelov, Dumitru Erhan, Vincent Vanhoucke, and Andrew Rabinovich. Going deeper with convolutions. In *Proceedings of the IEEE Conference on Computer Vision and Pattern Recognition (CVPR)*, June 2015.
- [28] Mingxing Tan and Quoc Le. EfficientNet: Rethinking model scaling for convolutional neural networks. volume 97 of *Proceedings of Machine Learning Research*, pages 6105–6114. PMLR, 2019.
- [29] Oriol Vinyals, Charles Blundell, Timothy Lillicrap, Koray Kavukcuoglu, and Daan Wierstra. Matching networks for one shot learning. In *Proceedings of the 30th International Conference on Neural Information Processing Systems*, NIPS'16, page 3637–3645. Curran Associates Inc., 2016.
- [30] Sandra Wachter, Brent Mittelstadt, and Chris Russell. Counterfactual explanations without opening the black box: Automated decisions and the gdpr. *Harvard Journal of Law and Technology*, 31(2):841–887, 2018.
- [31] Xiangyu Zhang, Xinyu Zhou, Mengxiao Lin, and Jian Sun. ShuffleNet: An extremely efficient convolutional neural network for mobile devices. In 2018 IEEE/CVF Conference on Computer Vision and Pattern Recognition. IEEE, jun 2018.

A Appendix

A.1 Training Details

A.1.1 Datasets.

We test our approach on image classification tasks using the Street View House Number (SVHN) dataset [21] (GNU 3.0 license), CINIC10 [4](MIT license) and CIFAR10 [13](MIT license). SVHN is a dataset containing $\sim\!\!73k$ images of house numbers in natural scenarios. The goal is to recognize the right digit in the image. Sometimes some distracting digits are present next to the centered digits of interest. CIFAR10 is an extensively studied dataset containing $\sim\!\!60k$ images where each image represents one of the 10 classes of the dataset. Finally, CINIC10 is relatively new dataset containing $\sim\!\!90k$ images that tries to bridge the gap betwen CIFAR10 and ImageNet in terms of difficulty, using the same classes of CIFAR10 and a subset of merged images from both CIFAR10 and ImageNet.

At the beginning of our experiments, we randomly extract from training sets a validation test of 6k images for each dataset. The images are normalized and, in CIFAR10 and CINIC10, we also apply an augmentation based on random horizontal flips. We do not use the random crop augmentation because, in some preliminary tests, it can hurt the performance, as a random crop can often isolate a portion of the image containing only the background. The memory in this case will retrieve similar examples based only on the background, pushing the network to learn useless shortcuts, degrading the performance.

The subsets of the training dataset to train models with 1000, 2000 and 5000 samples are extracted randomly and change in every run. This means that we extract 15 different subsets of the dataset and then test all the configurations on these subsets. We fixed the seed using the range (0,15) to make the results reproducible.

A.1.2 Training details.

The implementation of the architectures for our encoders f(x) starts from the PyTorch implementations of Kuang Liu³. To train the models, we follow the setup of Huang et al. [10], where they are trained for 40 epochs in SVHN and 300 epochs in CIFAR10. In both cases, we apply the Stochastic Gradient Descent (SGD) algorithm providing a learning rate that starts from 1e-1 and decreases by a factor of 10 after 50% and 75% of epochs. Note that this configuration is not optimal neither for baselines nor for Memory Wrap and you can reach higher performance on both cases by choosing another set of hyperparameters tuned in each setting. However, this makes quite fair the comparison across different models and datasets. We ran our experiment using a cloud hosted NVIDIA A100 and a GTX 3090.

Memory Set Regarding memory samples, in an ideal setting one should provide a new memory set for each input during the training process, however this makes both the training and the inference process slowe due to computational limits. We simplified the process by providing a single memory set for each new batch. The consequence is that performance at testing/validation time can be influenced by the batch size used: a high batch size means a high dependency on the random selection. To limit the instability, we fix a batch size at testing time of 500 and we repeat the test phase 5 times, extracting the average accuracy across all repetitions.

A.2 Final Layer.

In this section, we describe and motivate the choice of the parameters of the last layer. In principle, we can use any function as the last layer. In some preliminary tests, we compared a linear layer against a multi-layer perceptron. We found that linear layers require lower learning rates (in the range of [1e-2,1e-4]) to work well in our settings. However, for the considered datasets and models, the standard configuration requires a decreasing learning rate that starts from high values. To make the comparison fair, we choose, instead, a multi-layer perceptron that seems more stable and reliable at high learning rates. The choice of a linear layer is appealing, because it makes easier the inspection of the contribution of each sample in the memory to compute the final prediction, and in principle, one could obtain similar or higher results if hyperparameters are suitably tuned.

³https://github.com/kuangliu/pytorch-cifar

We use a multi-layer perceptron containing only 1 hidden layer. The input dimension of such a layer will be clearly $dim(l_f) = 2dim(e_{x_i})$ being $dim(e_{x_i}) = dim(\mathbf{v}_{\mathbf{S}_i})$ for the Memory Wrap and $dim(l_f) = dim(\mathbf{v}_{\mathbf{S}_i})$, for the baseline that uses only the memory vector. The size of the hidden layer $dim(h_{l_f})$ is a hyper-parameter that we fix multiplying the input size by a factor of 2.

A.3 Attribution Methods.

As described in the paper, it is possible to use an attribution method to highlight the most important pixels for both the input image and the memory set, with respect to the current prediction. The only requirement is that the attribution method must support multi-input settings. We use the implementation of Integrated Gradients [26] provided by the Captum library [12]. Note that, one of the main problems of these attribution methods is the choice of the baseline [26]: it should represent the absence of information. In the image domain, it is difficult to choose the right baseline, because there is a high variability of shapes and colors. We selected a white image as the baseline, because it is a common background on SVHN dataset, but this choice generates two effects: 1) it makes the heatmaps blind to white color and this means, for example, that heatmaps for white numbers on a black background focus on edges of numbers instead of the inner parts; 2) it is possible to obtain a different heatmap by changing the baseline.

A.4 Explanation Accuracy.

Table 7 shows the complete set of experiments for the computation of the explanation accuracy.

Table 7: Mean Explanation accuracy and standard deviation over 15 runs of the sample in the memory set with the highest sparse content attention weight.

0						
	Explanation Accuracy Memory Wrap %					
Dataset	Samples	EfficientNetB0	ResNet18			
SVHN	1000 2000 5000	86.09 ± 0.76 90.04 ± 0.51 93.19 ± 0.49	$69.85 \pm 3.29 84.64 \pm 2.02 92.45 \pm 0.26$			
CIFAR10	1000 2000 5000	80.06 ± 0.85 80.27 ± 0.57 85.05 ± 0.47	$72.95 \pm 1.00 78.42 \pm 0.58 85.86 \pm 0.46$			

A.5 Additional Architectures.

Table 8 and Table 9 show the performance of GoogLeNet [27], DenseNet [10], and ShuffleNet [31] on both datasets. We can observe that the performance trend follows that of the other architectures.

Table 8: Avg. accuracy and standard deviation over 15 runs of the baselines and Memory Wrap, when the training dataset is a subset of SVHN. For each configuration, we highlight in bold the best result and results that are within its margin.

	Reduced SVHN Avg. Accuracy%				
	Samples				
Model	Variant	1000	2000	5000	
GoogLeNet	Standard	25.25 ± 9.39	61.45 ± 16.56	88.63 ± 2.60	
	Only Memory	66.35 ± 6.93	87.10 ± 1.17	92.16 ± 0.28	
	Memory Wrap	$\textbf{74.66} \pm \textbf{9.01}$	$\textbf{88.32} \pm \textbf{0.78}$	$\textbf{92.52} \pm \textbf{0.25}$	
DenseNet	Standard	60.93 ± 9.21	83.47 ± 1.16	89.39 ± 0.60	
	Only Memory	40.94 ± 12.06	79.12 ± 5.36	$\textbf{89.69} \pm \textbf{0.63}$	
	Memory Wrap	$\textbf{73.69} \pm \textbf{4.20}$	$\textbf{85.12} \pm \textbf{0.62}$	$\textbf{90.07} \pm \textbf{0.49}$	
ShuffleNet	Standard	27.09 ± 6.05	60.05 ± 8.76	83.19 ± 1.00	
	Only Memory	$\textbf{32.22} \pm \textbf{3.47}$	60.06 ± 3.32	$\textbf{85.56} \pm \textbf{0.60}$	
	Memory Wrap	$\textbf{33.60} \pm \textbf{4.69}$	$\textbf{67.35} \pm \textbf{3.19}$	$\textbf{85.04} \pm \textbf{0.74}$	

Table 9: Avg. accuracy and standard deviation over 15 runs of the baselines and Memory Wrap, when the training dataset is a subset of CIFAR10. For each configuration, we highlight in bold the best result and results that are within its margin.

	Reduced CIFAR10 Avg. Accuracy%				
37.11	Samples				
Model	Variant	1000	2000	5000	
GoogLeNet	Standard	51.91 ± 3.14	63.90 ± 2.21	79.09 ± 1.28	
	Only Memory	54.25 ± 0.80	66.00 ± 1.27	79.65 ± 0.59	
	Memory Wrap	$\textbf{55.91} \pm \textbf{1.20}$	$\textbf{66.79} \pm \textbf{1.03}$	$\textbf{80.27} \pm \textbf{0.49}$	
DenseNet	Standard	46.99 ± 1.61	56.95 ± 1.68	73.72 ± 1.41	
	Only Memory	$\textbf{46.20} \pm \textbf{1.47}$	$\textbf{58.16} \pm \textbf{1.82}$	$\textbf{75.77} \pm \textbf{1.31}$	
	Memory Wrap	$\textbf{47.64} \pm \textbf{1.58}$	$\textbf{58.60} \pm \textbf{1.85}$	$\textbf{75.50} \pm \textbf{1.33}$	
ShuffleNet	Standard	$\textbf{37.86} \pm \textbf{1.16}$	45.85 ± 1.26	65.92 ± 1.54	
	Only Memory	$\textbf{38.15} \pm \textbf{1.14}$	$\textbf{48.91} \pm \textbf{2.12}$	70.05 ± 0.84	
	Memory Wrap	$\textbf{37.90} \pm \textbf{1.15}$	$\textbf{47.50} \pm \textbf{1.79}$	$\textbf{68.52} \pm \textbf{1.38}$	

Table 10: Avg. accuracy and standard deviation over 15 runs of the baselines and Memory Wrap, when the training dataset is a subset of CINIC10. For each configuration, we highlight in bold the best result and results that are within its margin.

Reduced CINIC10 Avg. Accuracy%					
	Samples				
Model	Variant	1000	2000	5000	
GoogLeNet	Standard	38.97 ± 1.16	47.83 ± 1.09	58.47 ± 0.91	
	Only Memory	40.77 ± 0.78	48.53 ± 1.05	57.86 ± 0.55	
	Memory Wrap	$\textbf{42.19} \pm \textbf{0.92}$	$\textbf{50.47} \pm \textbf{0.77}$	$\textbf{58.98} \pm \textbf{0.68}$	
DenseNet	Standard	36.33 ± 0.84	41.78 ± 0.92	52.63 ± 0.95	
	Only Memory	35.64 ± 1.18	42.77 ± 0.69	$\textbf{54.16} \pm \textbf{0.58}$	
	Memory Wrap	$\textbf{37.02} \pm \textbf{0.95}$	$\textbf{43.55} \pm \textbf{1.05}$	53.59 ± 0.61	
ShuffleNet	Standard	$\textbf{28.32} \pm \textbf{0.85}$	33.49 ± 0.93	46.36 ± 1.03	
	Only Memory	$\textbf{28.68} \pm \textbf{0.93}$	$\textbf{35.33} \pm \textbf{1.09}$	$\textbf{48.25} \pm \textbf{0.90}$	
	Memory Wrap	$\textbf{28.94} \pm \textbf{1.06}$	$\textbf{34.30} \pm \textbf{0.85}$	47.33 ± 1.34	

A.6 Computational Cost

In this section, we describe briefly the changes in the computational cost when adding the Memory Wrap.

A.6.1 Parameters.

The network size's increment depends mainly on the output dimensions of the encoder and on the choice of the final layer. In Table 11 we examine the case of an MLP as the final layer and MobileNet, ResNet18, or EfficientNet as the encoder. We replace a linear layer of dim (a,b) with a MLP with 2 layers of dimension $(a,a\times 2)$ and $(a\times 2,b)$ passing from a*b parameters to $a\times (a\times 2)+(a\times 2)\times b$. So the increment is mainly caused by the a parameter. A possible solution to reduce the number of parameters would be to add a linear layer between the encoder and the Memory Wrap that projects data in a lower dimensional space, preserving the performance as much as possible.

Table 11: Number of parameters for the models with and without Memory Wrap. The column *dimension* indicates the number of output units of the encoder.

Number of parameters				
Model	Dimension	Parameters		
EfficientNetB0	320	3 599 686		
Only Memory	-	3 808 326		
Memory Wrap	-	4 429 766		
MobileNet-v2	1280	2 296 922		
Only Memory	-	5 589 082		
Memory Wrap	-	15 447 642		
ResNet18	512	11 173 962		
Only Memory	-	11 704 394		
Memory Wrap	-	13 288 522		

A.6.2 Space complexity

Regarding the space required for the memory, in principle, we should provide a new memory set for each input during the training process. Let be m the size of memory and n the dimension of the batch, the new input will contain $m \times n$ samples in place of n. For large batch sizes and a large number of samples in memory, this cost can be too high. To reduce its memory footprint, we simplified the

process by providing a single memory set for each new batch, maintaining the space required to a more manageable m+n.

A.6.3 Time Complexity

Time complexity depends on the number of training samples included in the memory set. In our experiments we used 100 training samples for each step as a trade-off between performance and training time, doubling the training time due to the added gradients and the additional encoding of the memory set. However, in the inference phase, we can obtain nearly the same time complexity by fixing the memory set a priori and computing its encodings only the first time.

A.7 Impact of Memory Size

The memory size is one of the hyper-parameters of Memory Wrap. We chose empirically a value (100) that is a trade-off between the number of samples for each class (10), the minimum number of samples considered in the training set (1000), the training time and the performance. The value is motivated by the fact that we want enough samples for each class to get more representative samples for that class, but, at the same time, we don't want that often the current sample is also included in the memory set and the architecture exploits this fact.

Increasing the number of samples can increase the performance too (Table 12), but it comes at the cost of training and inference time. For example, an epoch of EfficientNetB0, trained using 5000 samples, lasts ~9 seconds when the memory contains 20 samples, ~16 seconds when the memory contains 300 samples and ~22 seconds when the memory contains 500 samples.

Table 12: Avg. accuracy and standard deviation over 5 runs of the configuration of Memory Wrap trained using different number of samples in memory, when the training dataset is a subset of SVHN.

Reduced SVHN Avg. Accuracy %					
Model	Samples	1000	Samples 2000	5000	
IVIOUCI	Samples	1000	2000	3000	
EfficientNetB0	20	64.95 ± 2.46	75.80 ± 1.17	84.86 ± 0.99	
	100	67.16 ± 1.33	77.02 ± 2.20	85.82 ± 0.45	
	300	66.70 ± 1.58	77.97 ± 1.34	85.37 ± 0.68	
	500	66.76 ± 0.98	77.67 ± 1.17	85.25 ± 1.02	
MobileNet	20	63.42 ± 2.46	80.92 ± 1.42	88.33 ± 0.36	
	100	68.31 ± 1.53	81.28 ± 0.69	88.47 ± 0.10	
	300	65.08 ± 0.30	82.05 ± 0.75	88.93 ± 0.37	
	500	69.88 ± 1.76	80.92 ± 1.74	88.61 ± 0.32	
ResNet18	20	39.32 ± 7.21	72.54 ± 3.03	87.30 ± 0.41	
	100	40.38 ± 9.32	74.36 ± 2.69	87.39 ± 0.45	
	300	44.42 ± 10.97	74.63 ± 3.28	87.75 ± 0.62	
	500	40.59 ± 12.27	76.97 ± 2.48	87.55 ± 0.35	

A.8 Uncertainty Detection.

Table 13 shows the accuracy reached by the models on inputs where the sample in memory associated with the highest weight is a counterfactual. In these cases, models seem unsure about their predictions, making a lot of mistakes with respect to classical settings. This behavior can be observed on $\sim 10\%$ of the testing dataset.

Table 13: Accuracy reached by the model on images where the sample with the highest weight in memory set is a counterfactual. The accuracy is computed as the mean over 15 runs.

Explanation Accuracy Memory Wrap %			
Dataset	Samples	EfficientNetB0	ResNet18
SVHN	1000 2000 5000	37.10 ± 1.45 40.77 ± 2.80 46.94 ± 1.49	31.10 ± 4.65 46.23 ± 1.74 50.04 ± 0.96
CIFAR10	1000 2000 5000	29.37 ± 0.84 35.44 ± 0.98 45.47 ± 0.90	31.74 ± 0.95 35.67 ± 1.25 42.17 ± 0.93

A.9 Additional Memory Images.

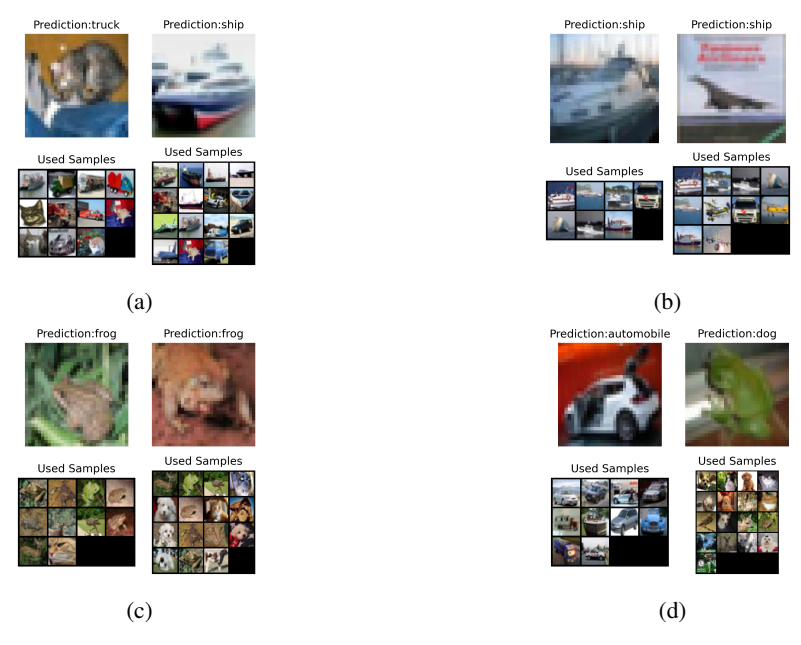


Figure 5: Inputs from CIFAR10 dataset (first rows), their associated predictions, and an overview of the samples in memory that have an active influence on the decision process - i.e. the samples from where the memory vector is built - (second row).



Figure 6: Inputs from SVHN dataset (first rows), their associated predictions, and an overview of the samples in memory that have an active influence on the decision process – i.e. the samples from where the memory vector is built – (second row).

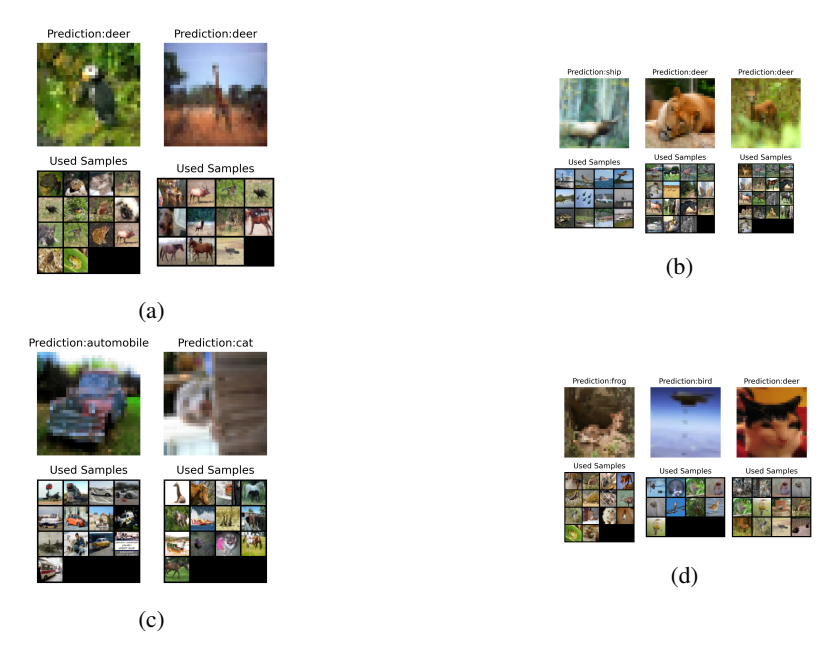


Figure 7: Inputs from CINIC10 dataset (first rows), their associated predictions, and an overview of the samples in memory that have an active influence on the decision process - i.e. the samples from where the memory vector is built - (second row).

A.10 Additional Heatmaps.



Figure 8: Heatmaps computed by the Integrated Gradients method for both the current input and the most relevant samples in memory on the CIFAR10 dataset.

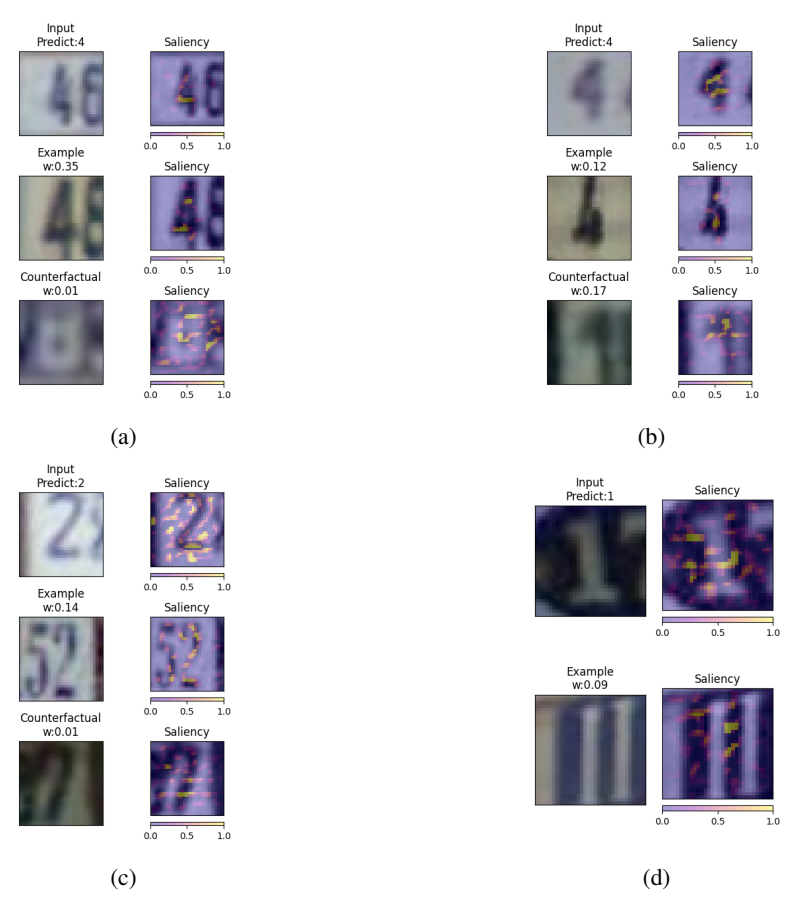


Figure 9: Heatmaps computed by the Integrated Gradients method for both the current input and the most relevant samples in memory on the SVHN dataset.



Figure 10: Heatmaps computed by the Integrated Gradients method for both the current input and the most relevant samples in memory on the CINIC10 dataset.